

# Letters

## Single crystal lamellar texture in a thin-walled cylindrical specimen of polyethylene

The purpose of this note is to describe our progress in making a specimen of oriented bulk polyethylene with a quasi single-crystal lamellar texture, not in the usual form of a sheet [1-3] or a disc [4, 5] but in a thin-walled hollow cylinder. To be precise, it is desired that (1) the orthorhombic crystal axes  $a$ ,  $b$  and  $c$  coincide respectively with the cylinder axes  $N$  (normal or radial),  $T$  (transverse or circumferential) and  $D$  (deformation) and (2) the crystal lamellae be stacked in layers with their normals ( $n_l$ ) parallel to  $D$ . This ideal lamellar orientation is shown schematically in Fig. 1 for a section of the cylinder wall.

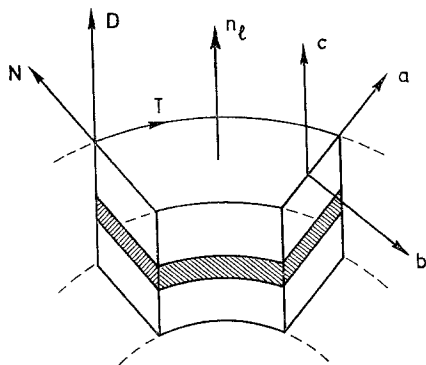


Figure 1 Section of a cylinder of polyethylene with an ideal single crystal lamellar texture. The crystallographic axes  $a$ ,  $b$  and  $c$  are parallel to the macroscopic axes  $N$ ,  $T$  and  $D$  and lamellar normals  $n_l$  parallel to  $D$ . The shaded region refers to interlamellar amorphous material.

The method of orienting the specimen is simply a variation of that of Seto and Hara [1]; by drawing a sheet at constant width a single-crystal texture is approached [1, 3]. Instead of starting with a sheet specimen we started with a short, thick-walled hollow cylinder and this was drawn at constant diameter. A flanged tube was machined from linear polyethylene (Hostalen GD6250, Farbwerke Hoechst AG), as shown in Fig. 2. Dimensions between flanges were: length

7.5 mm, i.d. 10 mm and wall thickness 1.8 mm. A circumferential notch (depth 0.25 mm) was cut at the centre of the section to initiate local necking. The tube was mounted in an Instron, and the assembly immersed in a thermostatted bath of glycerol. The tube was drawn at constant cross-head speed ( $4.2 \times 10^{-2}$  mm sec<sup>-1</sup>), at a bath temperature of 120°C, until the notched section was 18 mm long (a draw ratio of about 4:1). The cylinder was then annealed at 127°C for 1 h.

The crystallographic orientation was examined by wide angle X-ray pole figures using the 4-circle diffractometer technique described earlier [6]. The small sample used was cut from the centre of the tube (as in Fig. 2c) with the goniometer axis parallel to  $D$ . The reflection sphere

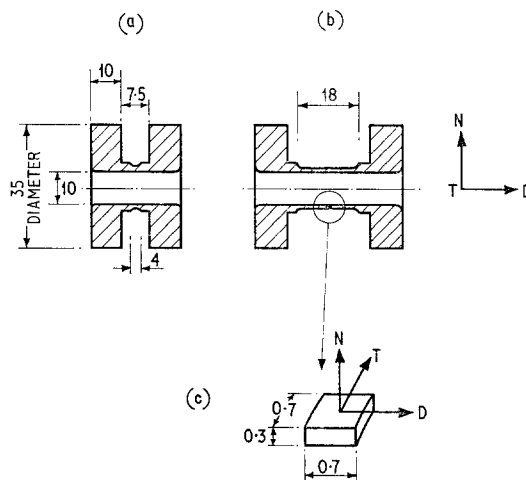


Figure 2 Sections through the flanged tube of polyethylene (a) before and (b) after being drawn on the Instron, together with (c) the sample cut out for the pole figure measurements. All dimensions are in mm.

was scanned by simultaneous increments  $\delta\chi$  ( $= 0.03^\circ$ ) and  $\delta\phi$  ( $= 10^\circ$ ) of the diffractometer angles  $\chi$  and  $\phi$ , where  $\chi$  (co-latitude) is the angle between pole  $I_{hkl}$  and  $D$ , and  $\phi$  (longitude) is the angle between  $N$  and the projection of  $I_{hkl}$  in the equatorial plane  $NT$ . The poles measured were (110), (200), (020) and (002), any two of which are sufficient to characterize the orientation in an orthorhombic crystal [7]. Shown in Fig. 3 are the combined (020) and (002) pole

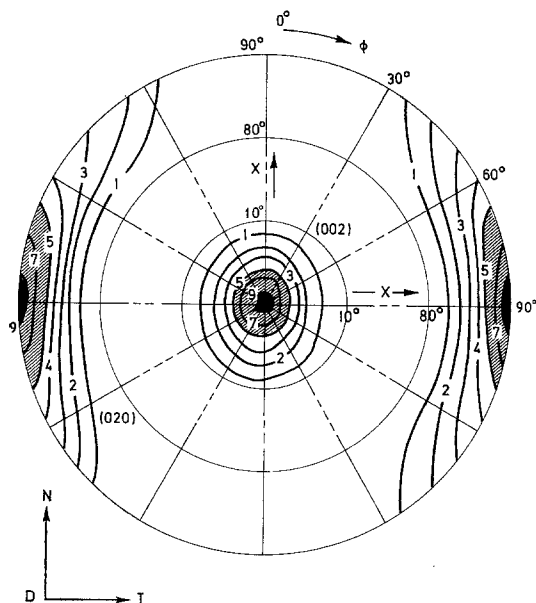


Figure 3 Combined wide-angle pole figures for (002) and (020) poles in a hot-drawn cylinder of polyethylene. (For explanation of contours and axes  $\chi$ ,  $\phi$ , see text.)

figures. The projection is the  $NT$  plane and the intensity contours (1, 2, 3, . . . , 9) represent 10, 20, 30, . . . , 90% of the intensity maximum for each pole. To display the distribution in the usual manner over a full hemisphere ( $\chi = 0^\circ$  to  $\chi = 90^\circ$ ) would obscure most of the contouring in such a highly oriented specimen. Thus Fig. 3 is drawn with a discontinuous  $\chi$  scale, the (002) poles being entirely mapped from  $0^\circ$  and  $10^\circ$   $\chi$  and (020) poles from  $80^\circ$  to  $90^\circ$   $\chi$ .

The (002) poles show a high degree of  $c$ -axis orientation parallel to  $D$ . The (020) poles show the required circumferential orientation of  $b$ -axes parallel to  $T$  but, as with sheet drawing [3] the spread of (020) poles is more pronounced in the equatorial plane than out of it. The (020) spread is an orientation effect and does not arise to any significant extent from the small ( $1^\circ$ ) variation in the direction  $T$  within the pole figure sample used. The (200) and (110) pole figures (not shown) are entirely consistent with the interpretation of a single-crystal texture having intensity maxima at, respectively,  $0^\circ$  and  $\pm 55^\circ$  to the radial direction  $N$ , though both poles (as with 020) are spread out in the  $NT$  plane.

The orientation of the specimen is best quantified by calculating the orientation functions  $f_{hkl,Z}$ , defined as  $\frac{3}{2} \langle \cos^2 \xi_{hkl,Z} \rangle - \frac{1}{2}$ , where

$\xi_{hkl,Z}$  is the angle between the principal poles (200), (020) and (002) and their associated directions ( $Z$ ) of preferred orientation, namely,  $N$ ,  $T$  and  $D$  respectively. In each case the average is computed over the appropriate intensity distribution. Thus, for perfect single-crystal orientation (Fig. 1)  $f_{200,N} = f_{020,T} = f_{002,D} = 1$ . (Note, since  $\xi_{002,D} = \chi$  the orientation function  $f_{002}$  [7] is equivalent to  $f_{002,D}$ , but  $f_{020}$  [7] does not equal  $f_{020,T}$ , rather  $f_{020,D}$ .) The results of spherical integration give for the polyethylene specimen  $f_{200,N} = 0.897$ ,  $f_{020,T} = 0.898$  and  $f_{002,D} = 0.986$ . These correspond to mean angular deviations from ideality of  $5\frac{1}{2}^\circ$  for  $c$ -axes and  $15^\circ$  for  $a$ - and  $b$ -axes.

The lamellar texture of the cylindrical specimen was examined by small angle X-ray scattering. With the beam parallel to  $N$ , the scattering pattern is a two-point pattern indicating [8] the usual alignment of lamellar normals ( $n$ ) parallel to  $D$  as required from Fig. 1.

The specimen described in this note is only a prototype but it does have all the essential features of the ideal texture. The reader may well ask why, apart from curiosity, such a cylindrical specimen of polyethylene should be sought in the first place? The answer is that it would be uniquely suitable for two reasons: (1) to study the  $\kappa$ -effect [9] and (2) to measure the crystal shear modulus  $C_{44}$ .

1. The response of linear polyethylene to rapid temperature increments or decrements is an initially enhanced creep rate, a phenomenon termed the  $\kappa$ -effect [9]. This is believed to be caused by induced thermoelastic stresses that arise from differential thermal expansion in the crystalline and amorphous components. The greater the anisotropy of thermal expansion ( $\alpha$ ), the greater should be the  $\kappa$ -effect. For the polyethylene crystal [10]  $\alpha_a^C = 2.3$ ,  $\alpha_b^C = 0.7$  and  $\alpha_c^C = -0.13 \times 10^{-4} \text{ }^\circ\text{C}^{-1}$ , while for amorphous material [11]  $\alpha^A = 3.4 \times 10^{-4} \text{ }^\circ\text{C}^{-1}$ . Now for a cylindrical specimen with the texture of Fig. 1, the largest difference in thermal expansion is in the circumferential direction  $T$  on the interface of crystal lamellae and amorphous inter-lamellar material. In torsional creep this direction ( $T$ ) is also that of the applied shear stress, and so a very large  $\kappa$ -effect is anticipated.

2. The nine components of the modulus tensor for orthorhombic polyethylene crystal have been calculated by Odajima and Maeda [12] at temperatures of 20 and  $-196^\circ\text{C}$ . More recently, McCullough and Peterson [13] have estimated

the temperature dependence of two of these components, the shear moduli  $C_{44}(T)$  and  $C_{55}(T)$ . These moduli refer to shear over (001) planes in the [010] and [100] directions, respectively. The two sets of calculations [12, 13] disagree over these moduli, for example at  $-196^{\circ}\text{C}$ ,  $C_{44}$  is quoted [12] as  $3.4 \times 10^{10}$  dyn  $\text{cm}^{-2}$  and [13] as  $4.5 \times 10^{10}$  dyn  $\text{cm}^{-2}$ , while the calculated  $C_{55}$  are 1.2 and  $2.3 \times 10^{10}$  dyn  $\text{cm}^{-2}$ , respectively. At present there is no experimental value for either  $C_{44}$  or  $C_{55}$ . Now torsion about the  $c$ -axis of a single crystal of orthorhombic symmetry involves [14] terms in  $C_{44}$  as well as  $C_{55}$ , but torsion around  $D$  of the cylindrical specimen of Fig. 1 will involve only the crystal modulus  $C_{44}$  together with  $G_A$ , the shear modulus of amorphous polyethylene. Thus from the measured composite shear modulus, the known crystallinity and the estimated [15] value of  $G_A$ , a series model calculation [16] would yield experimental values for  $C_{44}(T)$  to compare with the theoretical predictions.

Further work is under way in trying to improve the orientation; increasing the draw ratio to make a longer specimen will be the first step towards this, while it is also hoped to increase the transverse orientation function  $f_{020,T}$  from 0.898 towards the value of 0.972 reported for a disc specimen of single crystal texture [17]. The results of the experiments outlined above will be published elsewhere.

### Acknowledgements

The authors wish to thank Professor D. C. Phillips for the use of the diffractometer, Dr G. W. Groves for small angle X-ray photographs, and Drs N. G. McCrum and J. D. Campbell for useful discussions.

### References

1. T. SETO and T. HARA, *Repts. Prog. Polymer Phys. Japan* **9** (1966) 207.
2. I. L. HAY and A. KELLER, *J. Mater. Sci.* **1** (1966) 41; **2** (1967) 538.

3. C. P. BUCKLEY, R. W. GRAY and N. G. MCCRUM, *J. Polymer Sci. B* **8** (1970) 341.
4. R. J. YOUNG, P. B. BOWDEN, J. M. RITCHIE and J. G. RIDER, *J. Mater. Sci.* **8** (1973) 23.
5. R. J. YOUNG and P. B. BOWDEN, *ibid* **8** (1973) 1177.
6. E. P. CHANG, R. W. GRAY and N. G. MCCRUM, *ibid* **8** (1973) 397.
7. C. R. DESPER and R. S. STEIN, *J. Appl. Phys.* **37** (1966) 3990.
8. G. W. GROVES and P. B. HIRSCH, *J. Mater. Sci.* **4** (1969) 929.
9. J. M. HUTCHINSON and N. G. MCCRUM, *Nature, Physical Science* **236** (1972) 115.
10. G. T. DAVIS, R. K. EBY and J. P. COLSON, *J. Appl. Phys.* **41** (1970) 4316.
11. F. C. STEHLING and L. MANDELKERN, *Macromolecules* **3** (1970) 242.
12. A. ODAJIMA and T. MAEDA, *J. Polymer Sci. C* **15** (1966) 55.
13. R. L. MCCULLOUGH and J. M. PETERSON, *J. Appl. Phys.* **44** (1973) 1224.
14. R. F. S. HEARMON, in "An Introduction to Applied Anisotropic Elasticity" (Oxford University Press, Oxford, 1961) p. 49.
15. R. W. GRAY and N. G. MCCRUM, *J. Polymer Sci. A2* **7** (1969) 1329.
16. C. P. BUCKLEY, R. W. GRAY and N. G. MCCRUM, *J. Polymer Sci. B* **7** (1969) 835.
17. R. W. GRAY and R. J. YOUNG, *J. Mater. Sci.* **9** (1974) 921.

Received 11 September  
and accepted 25 October 1973

R. W. GRAY  
Department of Electronics  
and Electrical Engineering,  
The University, Glasgow, UK

J. M. HUTCHINSON  
Department of Engineering Science,  
Oxford University, Parks Road, Oxford, UK

J. F. MATHEWS  
Department of Chemical Engineering,  
University of Saskatchewan, Saskatoon,  
Saskatchewan, Canada

### Comments on "The equilibrium topography of sputtered amorphous solids"

Carter and his collaborators have reported a series of studies related to the equilibrium topography of sputtered amorphous solids [1-3].

In their recent work [3] the computer calculation has been devised to simulate the development of a general surface contour to the equilibrium condition. The purpose of this letter is to show that the two correction procedures described below should be introduced in their calculations and these corrections lead to the different